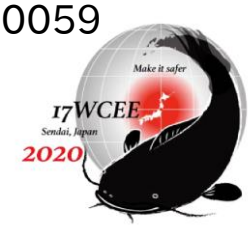

17th World Conference on Earthquake Engineering, 17WCEE
Sendai, Japan - September 13th to 18th 2020

SEISMIC BEHAVIOR OF UNBONDED POST-TENSIONED PRECAST CONCRETE WALLS WITH INTERNAL AND EXTERNAL DAMPERS

L. A. Bedriñana[(1)], M. Tani[(2)], S. Kono[(3)], M. Nishiyama[(4)]

[(1)] *Assistant Professor, Universidad de Ingenieria y Tecnologia - UTEC, lbedrinana@utec.edu.pe*
[(2)] *Associate Professor, Kyoto University, tani@archi.kyoto-u.ac.jp*
[(3)] *Professor, Tokyo Institute of Technology, kono.s.ae@m.titech.ac.jp*
[(4)] *Professor, Kyoto University, mn@archi.kyoto-u.ac.jp*
…

Abstract

In the last few decades, there has been a growing interest in applying unbonded post-tensioned (UPT) precast concrete structures in seismic regions to improve the seismic performance of concrete buildings by reducing the residual damage. Several experimental tests were conducted to investigate the structural performance of UPT walls. In most of the previous tests, UPT precast wall specimens showed a better performance compared to equivalent conventional structural walls. However, it has also been reported that the ultimate behavior of these UPT walls relies heavily on the detailing at their bottom joint, such as mechanical couplers for mild steel reinforcement and confining reinforcing details at their boundary elements. As a result, more research is needed on UPT precast concrete walls to evaluate their post-peak behavior and collapse potential. This paper presents the overview and results of an experimental investigation on the structural performance of UPT precast concrete walls subjected to reversed cyclic loads. In addition, this paper discusses the damage progression and failure mechanism of each specimen. Two half-scaled precast walls were investigated and each specimen consisted of two precast concrete panels joined only by post-tensioned unbonded strands. The bottom joint of each specimen had two types of damper: one specimen featured mild steel reinforcement crossing the bottom joint and the other specimen featured a set of hysteretic dampers attached to the wall surfaces. The hysteretic dampers were also fabricated from mild steel and had a buckling-restraining system. These dampers were set to contribute to the flexural capacity of wall specimens. A prestressing force of about 45% of the nominal yield strength of the strands was introduced to both specimens. In addition to the prestressing, a total axial load of 468.5 kN was applied to each specimen (axial load ratio of about 0.05), before any lateral loading. Fully reversed cyclic displacements were imposed on the wall specimens until a significant strength reduction was observed. Despite that significant axial loads were applied, both specimens sustained large lateral deformation (drifts above 3%) while maintaining their lateral strength, energy dissipation and self-centering capacity. A better performance was observed in the specimen with external dampers, with less residual drifts and less cover concrete spalling; moreover, the specimen with external dampers sustained larger lateral drifts (above 4%) without significant strength degradation. The external dampers were effective in dissipating energy until large drifts, where local buckling at the top end was observed; moreover, these dampers made an addition of about 15% for the equivalent damping ratio.

Keywords: post-tensioned; self-centering; shear walls; precast concrete; energy dissipater

© The 17th World Conference on Earthquake Engineering

1. Introduction

Over the last few decades, researchers have been investigating the advantages of Unbonded Post-Tensioned Precast (UPT) Wall Structures in seismic region. The main advantages of this system include sustaining large deformations while maintaining its lateral strength, energy dissipation, ability to self-center and controlled damage, limited to cover concrete spalling at the critical joint. Although some experimental efforts have been made to investigate the structural performance of UPT walls [1,2], there is limited information on UPT walls using external dampers. In addition, previous experimental research, on single-wall specimens, featured UPT walls with low levels of axial loads; then, further research is needed to evaluate the application of these walls as bearing structural walls.

In this study, an experimental test was conducted to evaluate the effects of external energy dissipation device on the post-peak behavior of UPT walls. Furthermore, this study intends to evaluate the collapse limit state of UPT walls (with internal and external energy dissipation) under high axial load ratios. More details of the specimens and test results can be found in Bedriñana, 2018 [3].

2. Specimens details

Fig. 1 shows the details of the test specimens. Two identical half-scaled UPT walls were investigated in this study: one featured internal energy-dissipating (ED) bars, and the other one, featured external dampers. Each specimen consisted of two precast concrete panels (1250x1485x125 mm) vertically joined by unbonded post-tensioning (PT) tendons. Other precast units (Anchor block, top, and bottom stubs) were also assembled by the PT tendons. In between two precast units, high strength mortar was cast to form a 15 mm thick joint.

Two tendons crossed the walls sections. Each of these tendons consisted of three Φ15.2 strands, located symmetrically at 100 mm from the wall´s centerline, and had a nominal yielding strength of $f_{py,n}$ = 1600 MPa. Two types of 7-wire strands were used: epoxy-coated strands (in specimen UPT-IA), and uncoated, low-relaxation strands (in specimen UPT-EA). The strands were fixed by multistrand anchorages that were located at the bottom of stub and at the top anchor block, providing a total unbonded length of 5.3 m. The initial prestressing force F_{po} was about 438 and 639 kN for specimens UPT-IA and UPT-EA, respectively. These forces correspond to a prestressing level ($f_{po}/f_{py,n}$) of 0.33 and 0.48 for specimens UPT-IA and UPT-EA, respectively. The differences in initial PT force was a product of the different response of the types of strands to the anchorages, i.e. epoxy-coated strands showed larger wedge movement during the post-tensioning.

The reinforcement of wall panels was identical in both specimens, except for the use of internal ED bars. Fig. 2.a) shows the reinforcement of the base panel (P1). A double mesh consisting of D6 bars spaced at 75 mm, in both the horizontal and vertical direction, was used as the main panel reinforcement. The boundary elements were confined by two high-strength steel hoops (S6-KSS785), spaced at 37.5 mm. The cover concrete in the panels was 15 mm.

As shown in Fig. 1, one specimen (UPT-IA) made use of a set of eight mild steel bars to connect the wall to the foundation, in addition to the PT reinforcement. These internal ED bars consisted of D13 bars, 4 bars at each side of the wall as shown in Fig. 2.a), that were deliberately unbonded over a length of 150 mm so to distributed yielding strains and to delay low-cycle fatigue fracture. The unbonded length of ED bars was located at the bottom joint, just at the beginning of the joint mortar. Each ED bar was connected by a grouted sleeve splice at the bottom joint, the splices were allocated on the bottom stubs prior to the assembling of precast units, to provide continuity with reinforcement at the foundation. As it was originally proposed [1], the internal ED bars are intended to concentrate yielding deformation; thus, providing energy dissipation capacity to the systems, for which they should not fracture prematurely.

Fig. 2b) presents the main features of the external dampers used in specimen UPT-EA. The external hysteretic dampers were machined from 20 mm anchor bolts to 13 mm, over a fused length of 150 mm, so to make a direct comparison with specimen UPT-IA. Since these dampers are expected to undergo compressive

© The 17th World Conference on Earthquake Engineering

stresses during gaps closing, which eventually may lead to premature buckling of the steel bars, a steel tube (with an outside diameter of 27 mm and a thickness of 3 mm) was located over the fused length of the damper. In addition, the steel tube was filled with non-shrinking grout. This grouted steel tube system is intended to delay buckling of the fused length, allowing the dampers to yield under tension and compression, even at large walls' drifts. The external dampers were attached to the specimens via strong steel connectors (Fig. 2.b), which were designed to allow quick installation and replacement of the dampers. The steel connectors were fixed to the wall panel by high-strength bolts that passed through the panel section. which were post-tensioned so to avoid any slippage.

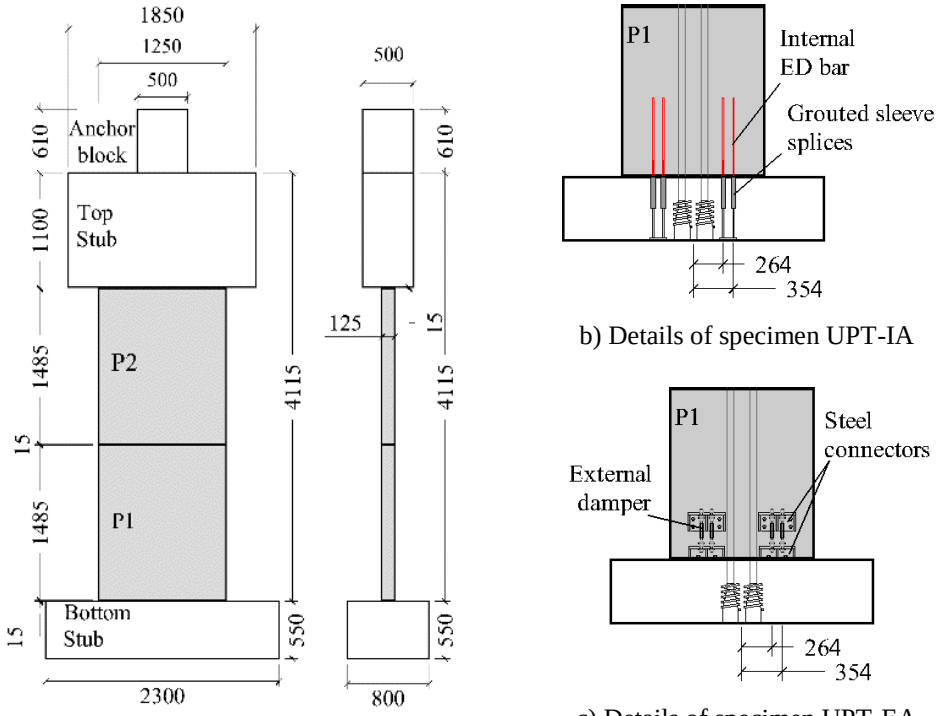

a) Dimensions (units: mm)

b) Details of specimen UPT-IA

c) Details of specimen UPT-EA

Fig. 1 – Details of test specimens

Table 1 shows the measured properties of the concrete used for the panels. The specified concrete strength for all precast units was 60 MPa; however, the measured values of f'_c for precast panels were above 80 MPa. The measured compressive strength of concrete for stubs was about 91 MPa, and the compressive strength of the joint mortar was 102 MPa. Moreover, the measured compressive strength of the dampers grout was 69.4 MPa.

Table 2 presents the average values of the reinforcing bars' material properties. The yielding strength of panel reinforcement and hoops was 403.7 and 889.0 MPa, respectively. Note that high-strength hoops were used to improve the efficiency of confinement and to reduce the required volumetric ratio at the boundary elements. The internal ED bars had a yielding strength of 387.0 MPa, whereas the external hysteretic dampers showed a yielding strength of about 360.8 MPa. As for the PT reinforcement material properties, two types of strands were used and the measured values of tensile strength (f_{pu}) were 1992.7 and 1910.3 MPa for the epoxy-coated and uncoated strands, respectively; moreover, the measured values of yielding strength (f_{py}), calculated as the 0.2% offset stress, was 1824.5 and 1803.6 MPa for the coated and uncoated strands, respectively.

© The 17th World Conference on Earthquake Engineering

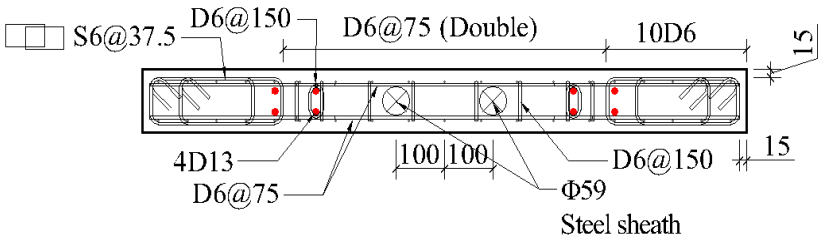

a) Base panel reinforcement

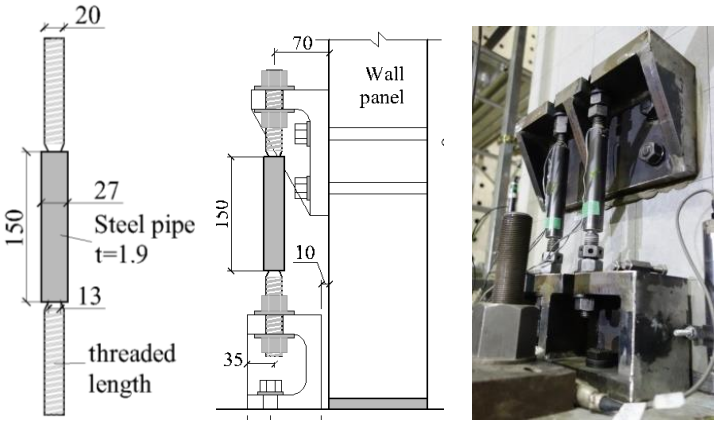

b) Details of external replaceable dampers

Fig. 2 – Details of test specimens

Table 1 – Material properties of concrete

Specimen	Panel P1			Panel P2		
	f'_c (MPa)	f'_t (MPa)	E_c (MPa)	f'_c (MPa)	f'_t (MPa)	E_c (MPa)
UPT-IA	83.8	3.8	37765	84.9	-	38863
UPT-EA	85.2	5.4	37047	89.7	5.8	39231

Note: Presented values are the average of at least three samples

Table 2 – Material properties of steel reinforcing bars

Type	f_y (MPa)	f_u (MPa)	E_s (x10^5 MPa)
Panel reinforcement	403.7	519.7	1.937
Hoops	889.0	1019.4	1.803
Internal Dampers	387.0	550.9	1.850
External Dampers	360.8	563.6	2.043

Note: Presented values are the average of at least three samples

© The 17th World Conference on Earthquake Engineering

3. Test setup

The loading setup for the experiment can be seen in Fig. 3. Horizontal loads were applied by a servo-controlled, 3000 kN-capacity hydraulic jack, which was attached to the specimen top stub by a rigid steel jig. The lateral loads were applied at a level of 3265 mm from the bottom joint. The vertical load was applied by two 1000 kN vertical jacks. A total axial load of 468.5 kN (which represents an axial load ratio of 0.05) was applied to the specimen, prior to any lateral load application, and kept constant throughout the test. After the axial load was applied, displacement-controlled, fully reversed cyclic loads were applied to the specimen with peak drifts of 1/6000, 1/800, 1/400, 1/200, 1/100, 1/50, 1/33, 1/25 and 1/20 rad. Two full cycles were applied at each peak drift, except for 1/6000 drift where only one cycle was applied. The loading was stopped when a strength degradation of above 20% of the maximum lateral load was observed or after a drift of 5%.

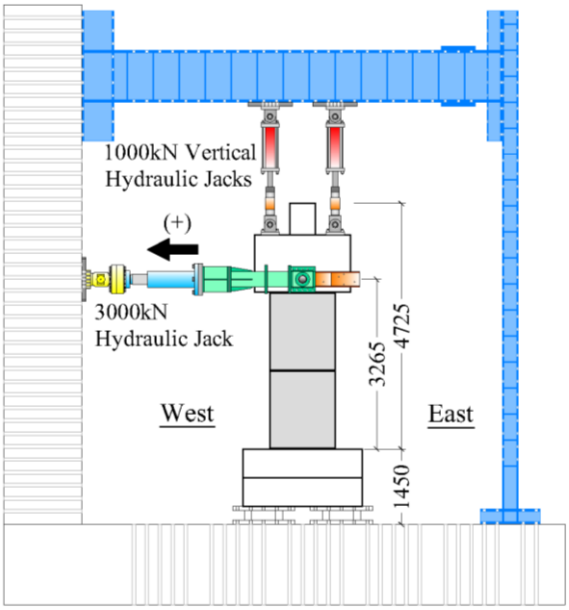

Fig. 3 – Details of test specimens

4. Test results

Fig. 4 shows the measured base shear force-drift behavior of the specimens, with the observed limit states also indicated. Despite the total axial load ratio, due to gravity loads, vertical loads, and prestressing force, being considerable (0.07 for UPT-IA and 0.08 for UPT-EA), both specimens sustained drifts larger than 3% without significant strength degradation and with minor damage. The peak shear force was 301 and 320 kN at -3% drift for UPT-IA and UPT-EA, respectively. After achieving the peak shear force, strength degradation was observed due to the fracture of either internal ED bars or external dampers.

Fig. 5 shows the final condition of the specimens. Damage in the specimens was limited to the base panel and no damage was observed on the upper panel. Gap opening became visible from 0.125% drifts as a crack at the base joint for both specimens. Moreover, minor flexural cracks started to appear on the surface of the base panel at 0.25% drift for both specimens, but they fully closed when the specimens were unloaded. Cover concrete spalling was initially observed at drifts of 1% in both specimens, and by the end of the test, cover concrete spalling was limited to a relatively small area at the toes of the wall (about 400 mm long and 150 mm high for UPT-IA). Nevertheless, it was observed that the core concrete and confinement hoops were sound after the test, making the boundary elements still able to sustain the axial load. Moreover, the crushing of the base joint mortar was observed after 3% drifts.

© The 17th World Conference on Earthquake Engineering

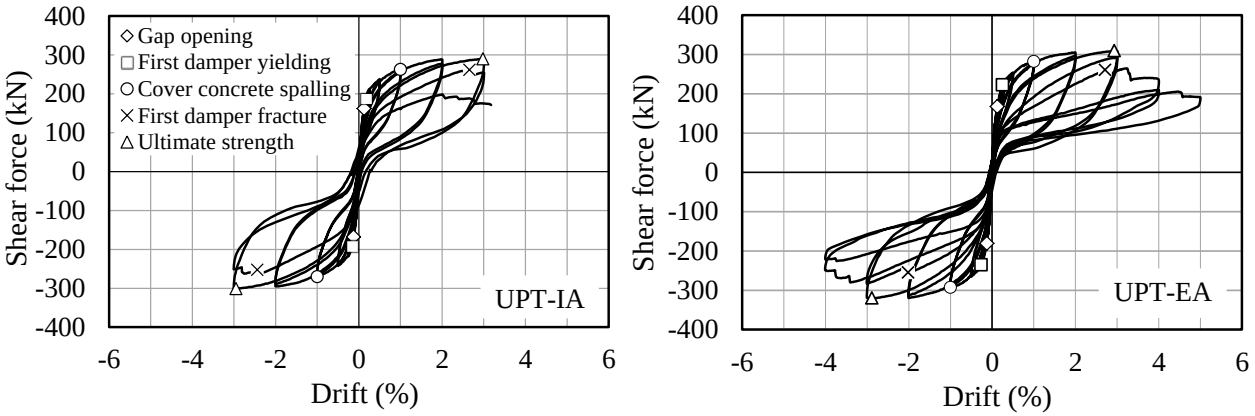

Fig. 4 – Load-Deformation behavior of test specimens

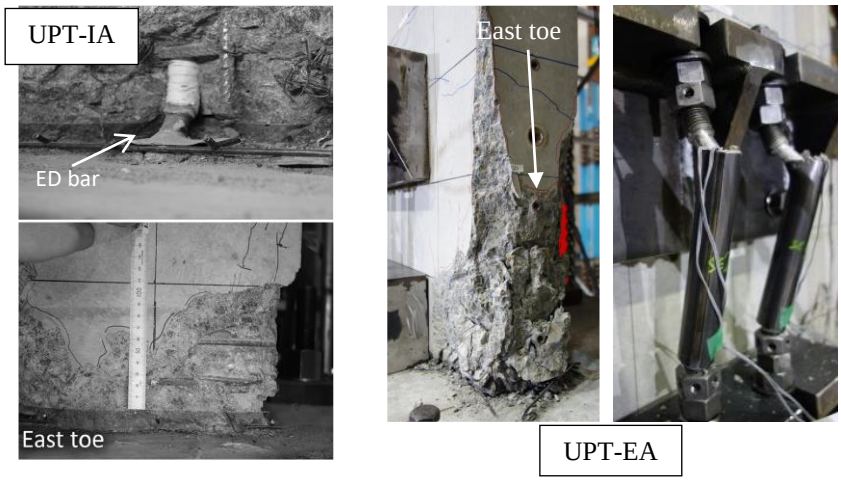

Fig. 5 – Final condition of specimens

The yielding of ED bars and external dampers provided the main source of energy dissipation in their corresponding specimen. The ED bars of specimen UPT-IA started to yield at 0.17% drift, whereas external dampers started to yield at 0.25% drift on UPT-EA. Buckling of the unbonded length of ED bars was noted at large drifts, 2nd cycle at 3%, prior to fracturing, which pushed the surrounding concrete outward and caused unexpected cover concrete spalling at the center of the base panel (See Fig. 2). This buckling of ED bars also caused an out-of-plane displacement (to the north) of UPT-IA, which reached a large as 20 mm by the end of the test. One of the ED bars (at the east side) fractured first during the 2nd cycle of the 3% drift in UPT-IA and was followed by three more bars, which fractured on the way to the next peak drift of the 4% drift. This fracture of the ED bars caused a strength degradation of more than 30% of the peak load and resulted at the end of the test. The significant buckling can be considered as the reason for the earlier fracture of ED bars compared to the external dampers, and the out-of-plane displacement, in addition to the earlier fracture of dampers, is attributed as the main cause for the significant strength degradation in specimen UPT-IA.

Despite using steel tubes, the external dampers also suffer from localized flexural buckling, at the top end (see Fig.5), before fracturing. However, all the dampers fractured under tensile stresses, after providing considerable energy dissipation. Moreover, the external dampers could be replaced after the test. The first external damper, at the east side of UPT-EA, fractured during the 1st cycle of the 4% drift and was immediately followed by two more dampers, which fracture in the same cycle, causing a strength degradation below 30%. After this, one more loading cycle, until 5% peak drift, caused the fracture of the last damper on the east side of UPT-EA. After the test, all the fractured dampers could be removed easily,

© The 17th World Conference on Earthquake Engineering

which allows a quick replacement, if necessary, and validates the design of the damper and connector configurations.

Fig. 6 shows the measured PT tendon stresses. The PT tendons provided the main restoring force to the specimens and it was observed that they remained within the elastic range (yielding strength was 1803MPa) throughout the test. There was some loss in the PT force, which can be attributed to the strand-anchorage interaction and the damage of the bottom joint mortar. The maximum prestress loss was about 10% for UPT-IA and 20% for UPT-EA of the initial prestressing force. It has been reported that certain PT anchorages may cause the premature fracture of PT strands when they are subjected to cyclic inelastic stresses [4,5]. In this test, the PT anchorages performed adequately, preventing premature fracture of tendons, mainly because the stresses in the tendons were below the yield strength, as it was designed.

The measured values of relative energy dissipation ratio are shown in Fig. 7. The relative energy dissipation ratio β, as defined in the ACI ITG-5.2 [6], was used to quantify the amount of energy dissipation of the specimens. It is required that β should be no less than 0.125 at the maximum strength level so to ensure [6]. It was observed that both ED bars and external dampers provided an adequate amount of energy dissipation to the specimens until their peak strength was reached. UPT-IA showed larger β than UPT-EA, which can be attributed to the larger contribution of the cover concrete due to the ED bar buckling. Nonetheless, the use of external dampers in UPT-EA resulted in less concrete spalling and provided a quick replacement of dampers after the test, which is critical to restoring the capacity on UPT walls after a severe earthquake.

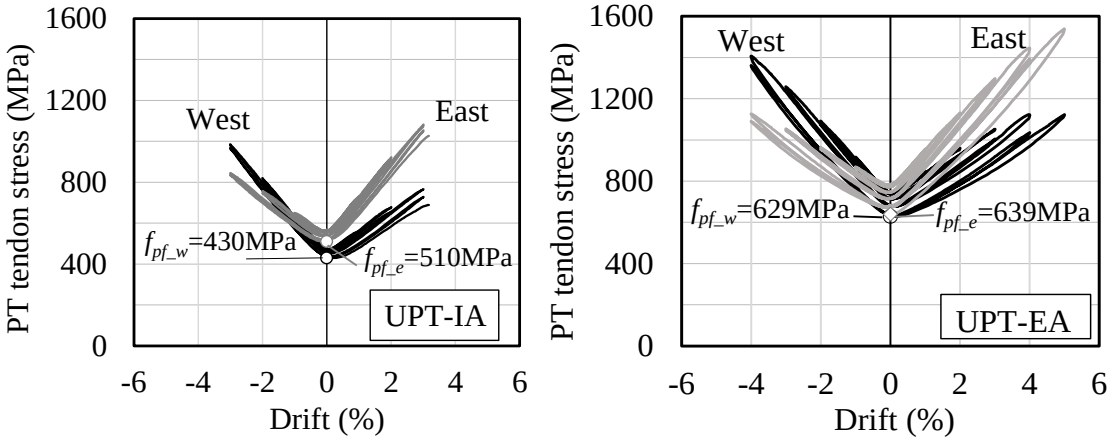

Fig. 6 – Stresses variation in PT tendons

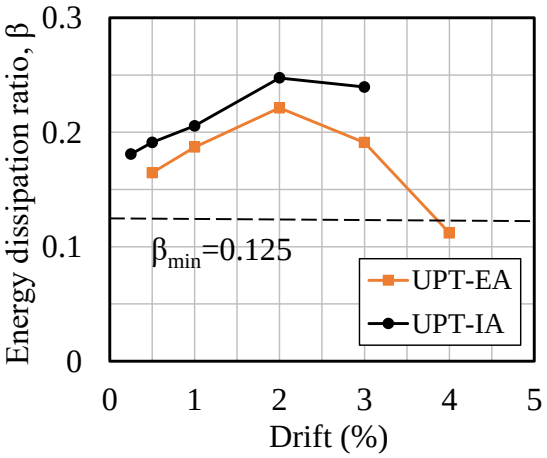

Fig. 7 – Values of relative energy dissipation ratio

© The 17th World Conference on Earthquake Engineering

Fig. 8 presents the values of gap opening displacement at the sides of specimens, measured at the bottom joint. As expected, the gap opening at the bottom joint was extensive and concentrated on the inelastic deformations of the specimens. The maximum gap opening was 30 and 52 mm for UPT-IA and UPT-EA, respectively. The differences in gap opening were mainly due to the different initial prestressing force introduced to the specimens. The upper panel-to-panel joint opening was minor for UPT-EA, with a peak value of about 1.7 mm. On the contrary, specimen UPT-IA showed a peak value of gap opening, at the sides of the middle joint, of about 3 mm. This large opening at the middle joint of UPT-IA can be attributed to the lower PT force introduced to the wall, compared to the initial prestress applied to UPT-EA. Then, an adequate initial PT force should be applied to UPT walls in order to limit the openings at upper joints. However, the gap openings at middle joints were fully closed after the unloading of the specimens.

The residual drifts after each peak drift are plotted in Fig. 9. Due to the use of unbonded PT tendons, the specimens were able to self-center with residual drifts smaller than 0.30 and 0.09% for UPT-IA and UPT-EA, respectively. It is important to mention that these small residual drifts were obtained despite achieving the ultimate strength and after the energy-dissipation mechanism fractured. Moreover, UPT-IA showed three times larger residual drifts than UPT-EA, mainly due to the lower initial prestress and the difficulty in closing bottom joint gaps after the buckling of ED bars. Then, external dampers can be considered more efficient for recovering after a severe earthquake.

5. Conclusions

Two identical, half-scaled, UPT walls, each with different damper configuration, were tested to evaluate their seismic performance and post-peak behavior. Despite significant axial loads were applied, the test specimens performed as expected: they sustained large lateral deformation, while maintaining lateral strength, with adequate energy dissipation and self-centering capacity. Both types of dampers provided adequate energy dissipation capacity, with values of β large than 0.125 until the peak strength. However, a better performance was observed in UPT-EA, in terms of less residual drifts, less cover concrete spalling, and larger drift capacity. In addition, UPT-EA showed the advantage of quick capacity recovery after earthquakes by simply remove and replace the external dampers.

The failure of the test specimens was determined by the fracture of the dampers. The internal ED bars in UPT-IA buckled significantly prior to their fracture, causing out-of-plane displacements, larger concrete cover spalling at the bottom joint, and larger residual drifts than in UPT-EA. On the other hand, the external dampers were effective in dissipating energy until large drifts (above 3%), after which localized flexural buckling at the top end was observed. Even though both specimens showed adequate energy-dissipation, UPT-EA had the advantage of replaceable external dampers, which more suitable for quick post-earthquake recovery.

The confinement details provided to the specimens showed to be adequate since the core concrete of the boundary elements remained sound even after the test, despite the considerable cover concrete spalling at the toes. However, the bottom joint mortar sustained some crushing, producing prestress losses on the specimens. The PT tendons remained under the elastic range in both specimens, which was an important factor to keep small residual drifts and to prevent any premature fracture of strands. However, different initial prestressing forces between specimens produced different gap openings at the bottom joint.

6. Acknowledgments

The tests presented in this paper were financially supported by the Japan Society for the Promotion of Science (JSPS) through its Grants-in-Aid for Scientific Research program (KAKENHI), Grant Numbers 16K06572 (Principal Investigator: M. Tani) and 16H02373 (Principal Investigator: S. Kono). In addition, Sumitomo (SEI) Steel Wire Corp., Splice Sleeve Japan, Ltd., Haiko-Honten Co., Ltd., P.S. Mitsubishi Construction Co., Ltd., and Sumikura-kozai Co., Ltd. supported the construction of test specimens. The assistance of Kaiwei Zhang, Duc Quang Tran, and Sakie Shiotani, former students at Kyoto University, is

© The 17th World Conference on Earthquake Engineering

appreciated. The first author thanks the financial support of CONCYTEC/CIENCIACTIVA for his doctoral studies at Kyoto University, where this research was conducted.

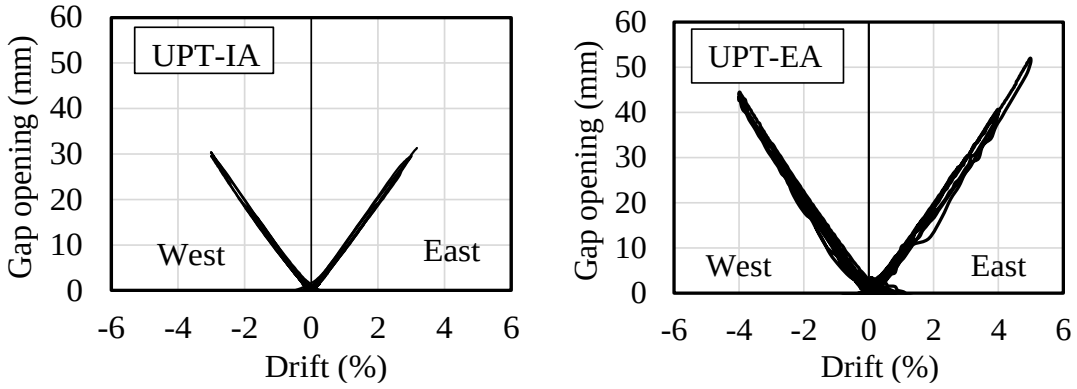

Fig. 8 – Values of gap opening displacement at the sides of the bottom joint

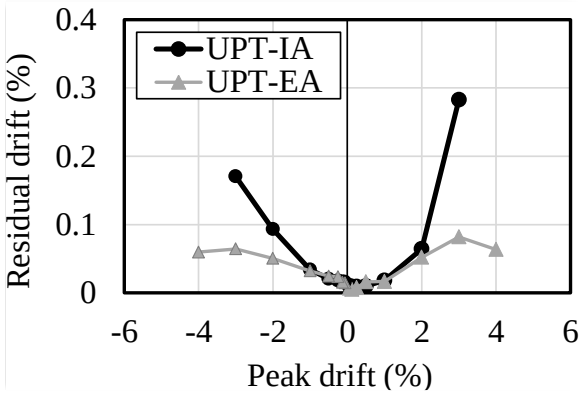

Fig. 9 – Values of residual drifts

7. References

[1] Smith BJ, Kurama YC, McGinnis MJ. Behavior of Precast Concrete Shear Walls for Seismic Regions: Comparison of Hybrid and Emulative Specimens. J Struct Eng 2013;139:1917–27. doi:10.1061/(ASCE)ST.1943-541X.0000755.

[2] Restrepo JI, Rahman A. Seismic Performance of Self-Centering Structural Walls Incorporating Energy Dissipators. J Struct Eng 2007;133:1560–70. doi:10.1061/(ASCE)0733-9445(2007)133:11(1560).

[3] Bedriñana LA. Seismic Performance and Seismic Design of Damage-Controlled Prestressed Concrete Building Structures. PhD Thesis, Kyoto University; 2018. doi:10.14989/doctor.k21364.

[4] Weldon BD, Kurama YC. Nonlinear Behavior of Precast Concrete Coupling Beams under Lateral Loads. J Struct Eng 2007;133:1571–81.

[5] Bedriñana LA, Zhang K, Nishiyama M. Evaluation of the behavior and ultimate capacity of unbonded monostrand-anchorage systems under concentric and eccentric inelastic cyclic loading. Eng Struct 2018;176:632–51. doi:10.1016/J.ENGSTRUCT.2018.09.036.

[6] ACI ITG-5.2-09. Acceptance Criteria for Special Unbonded Post-Tensioned Precast Structural Walls Based on Validation Testing. ACI ITG 5.1-07, The American Concrete Institute (ACI), Farmintong Hills, MI; 2007.

© The 17th World Conference on Earthquake Engineering